Narrow log-periodic modulations in non-Markovian random walks

R. M. B. Diniz,[1] J. C. Cressoni,[2,3] M. A. A. da Silva,[2] A. M. Mariz,[1] and J. M. de Araújo[1]
[1]*Departamento de Física Teórica e Experimental, Universidade Federal do Rio Grande do Norte, Natal, RN, 59078-900, Brazil*
[2]*Departamento de Física e Química, FCFRP, Universidade de São Paulo, 14040-903 Ribeirão Preto, SP, Brazil*
[3]*Instituto de Física, Universidade Federal de Alagoas, Maceió, AL, 57072-970, Brazil*
(Received 10 October 2017; published 26 December 2017)

What are the necessary ingredients for log-periodicity to appear in the dynamics of a random walk model? Can they be subtle enough to be overlooked? Previous studies suggest that long-range damaged memory and negative feedback together are necessary conditions for the emergence of log-periodic oscillations. The role of negative feedback would then be crucial, forcing the system to change direction. In this paper we show that small-amplitude log-periodic oscillations can emerge when the system is driven by positive feedback. Due to their very small amplitude, these oscillations can easily be mistaken for numerical finite-size effects. The models we use consist of discrete-time random walks with strong memory correlations where the decision process is taken from memory profiles based either on a binomial distribution or on a delta distribution. Anomalous superdiffusive behavior and log-periodic modulations are shown to arise in the large time limit for convenient choices of the models parameters.

DOI: 10.1103/PhysRevE.96.062143

I. INTRODUCTION

The first observations of diffusion were reported by Jan Ingen-Housz in 1784 by observing the erratic motion of powdered charcoal floating on an alcohol surface [1]. The phenomenon, however, was named Brownian motion (BM) after Robert Brown's investigations in 1828 [2] on the movements of fine particles, including pollen, dust, and soot, on a water surface. Diffusion models were later used to describe transport phenomena, starting with the seminal work of Einstein [3] and von Smoluchowski [4], establishing the theoretical basis for the study of the diffusion processes and its relation to the underlying microscopic particle dynamics [5]. Since then, the statistical description of diffusion processes have often been studied by the use of random walks (RW) [3,4,6–8] and/or stochastic differential equations. These approaches are different but complementary. The first approach, based on the theory of random walks [9,10], is a concept that is closely related to the development of Brownian motion [3] (see history and references in Refs. [5,11–17]). The second approach relies on the use of stochastic differential equations [16] which includes the use of the Langevin equation [18] along with the generalized Langevin equation [19–21], continuous-time random walks (CTRWs) [10,13,22,23], and the fractional Fokker-Planck method [24,25].

Transport dynamics in complex systems is governed by anomalous diffusion. Such anomalous transport processes are associated with a diffusing particle for which the variance spreads in nonlinear fashion with time [26], i.e., $\langle x^2 \rangle - \langle x \rangle^2 \sim t^{2H}$. The Hurst exponent H is then associated to subdiffusive ($H < 1/2$) and superdiffusive ($H > 1/2$) dynamics ($H = 1/2$ corresponds to normal diffusion). For the RW models we consider in this paper, the mean squared displacement (MSD) satisfies $\langle x^2(t) \rangle \sim \langle x^2 \rangle - \langle x \rangle^2 \sim t^{2H}$. Anomalous diffusion is exhibited by many systems in nature such as, physics, chemistry, geophysics, biology, and economy [12,24,27–38]. Another interesting class of diffusion behavior is the ultraslow diffusion, also termed *strong anomalous diffusion*, in which the MSD grows logarithmically with time, i.e., $\langle x^2 \rangle \sim (\ln t)^\kappa$, with $\kappa > 0$. Examples of this behavior can be found, for example, in the Sinai model [39], diffusion on random structures with a topological bias [40], random walks on bundled structures [41], diffusion in periodic iterated maps [42] and in non-Markovian random walk with pauses [43].

Theoretical models describing anomalous diffusion often incorporate memory effects [13,23,29,44], like the elephant random-walk (ERW) model [45], which consists of a random walker whose decisions depend on its entire history of previous decisions. Several modifications and reformulations of the ERW have been proposed in the literature [46–50]. The model in this study follows closely the same dynamics of the ERW model but uses a memory profile that restricts the memory available to the walker. Restricted memory impersonates memory damage in the sense that only part of the memory is used for decision making. The use of damaged memory has been shown to give rise to new interesting phenomena such as negative feedback persistence and log-periodicity [46]. The latter is directly associated with a breakdown of the continuous scale-invariance (CSI) symmetry into a discrete scale invariance (DSI) symmetry [51]. The diffusive behavior at large times depends entirely on the details of the memory pattern governing the decision process. In this paper we consider a non-Markovian random walk driven by a binomially distributed discrete memory profile. Several reasons led us to choose this particular memory pattern. First, with this choice the memory profile can be fully controlled by an internal parameter, which simplifies the overall analysis of the diffusion processes. External parameters can be used to characterize the memory function but they are often very cumbersome to deal with. An inherent and easily controllable memory size, for example, is very convenient for analytical studies, being especially useful for analyzing the asymptotic limit. Besides, with the binomial function, the time position of the most probable memory accessed by the walker is also regulated internally by the same parameter that fixes the size of the memory. Second, the binomial distribution provides an effective memory size that shortens as time progresses, leading to a δ function in the asymptotic limit. This kind of

dynamical behavior of the memory size is somewhat unusual, which makes the binomial memory an interesting case to study. Besides, continuous-time results for the δ memory profile are already known [52], which we use as an aid in the large time analysis of the binomial model. Finally, another reason for using the binomial function to model the memory profile is due to the fact that it is discrete. Therefore, once normalized, there is no need to use a cutoff to avoid the function to spread outside the time interval $[0,t]$. Although we do not provide a general analytic solution for the binomial profile memory model, we do provide an exact solution for the first moment in the asymptotic limit. The results indicate the presence of log-periodic oscillations, both in the normal and superdiffusive regimes, within regions of the phase diagram associated with negative and positive feedback. The oscillations associated with positive feedback are of very small amplitude and totally nonexpected. Small relative log periodic corrections have been reported before [53–55] and renormalization group approaches have been used to study their appearance in critical behavior [56,57]. As far as we know they have never been reported before in non-Markovian random walks with an explicit memory dependence. In this paper we provide an exact discrete-time solution to explain the origin of the oscillations. This study allows us to enhance our understanding about the source of log-periodic modulations in random-walk transport phenomena and their relations with long-range memory-correlated models. In Sec. II we describe the models and the corresponding memory profiles. A discrete-time solution for the first moment of the δ memory profile is also derived. Section III presents the results and in Sec. IV we discuss and conclude.

II. THE MODELS

We consider a one-dimensional random walker initially positioned at $X_0 = 0$ at time $t = 0$ and at position X_t at time t. At time $t + 1$ the walker moves to the left or right with a unitary step, i.e., $X_{t+1} = X_t + \sigma_{t+1}$, where $\sigma_{t+1} = \pm 1$. The choice of σ_{t+1} depends on the decision taken at a randomly chosen earlier time t' which is chosen, *a priori*, from a distribution that characterizes the memory pattern (or memory profile) of the model. We make use of two memory profiles, namely the binomial memory profile and the δ memory profile, as described below.

A. The binomial memory profile

In the binomial memory profile model a random earlier time t' is chosen, *a priori*, from a binomial distribution, i.e.,

$$P_r(t',t) = \binom{t}{t'} r^{t'}(1-r)^{t-t'} \tag{1}$$

for $r > 0$. We fix $t' = 0$ for $r = 0$ and $t' = t$ for $r = 1$. The parameter r represents the probability of success in the binomial distribution. In the model, r is associated with the geometric center of the distribution of available memory, since $\langle t' \rangle = rt$. Note that in the ERW model [45] t' is chosen from a uniform distribution, with $0 \leqslant t' \leqslant t$. The binomial profile model allows better control of the memory size and its position in the chain of past events. Besides, past events are no longer equivalent, some being more promptly remembered than others. The rest of the dynamics follows the same steps defined in the ERW model. At time $t + 1$, the walker chooses to repeat the previous decision taken at time t' with probability p (in which case we set $\sigma_{t+1} = \sigma_{t'}$) or to refuse it with probability $1 - p$ (in this case we set $\sigma_{t+1} = -\sigma_{t'}$).

According to these rules the parameter p governs the dynamics and provides positive (negative) feedback for $p > 1/2$ ($p < 1/2$). The traditional random walk (or Brownian motion) with normal diffusion is also recovered for $p = 1/2$, as usual. The binomial model incorporates a very convenient bonus, namely that distant and recent memories are readily distinguished by the parameter r, i.e., for r close to 1 recent memories are accessed more often than distant memories. The opposite occurs when r is close to zero, in which case distant memories are more common. This is a distinctive property of the model that immediately allows the study of either the distant or recent memory cases by simply switching a single parameter of the model.

The binomially distributed memory model does not have yet a known exact solution. However, we can find an approximate solution by mapping the model onto an equivalent rectangular memory profile model [58–60]. We assume that such a mapping can be done, which is supported by the numerical results below. The rectangular memory profile model has an effective rectangular memory of size $L \equiv L(r,t)$ and is centered in the most probable value of t'. Since the distribution is discrete we have to go to the continuum limit by interpolation. The probability of choosing a previous t' is now given by $1/L$. The memory that can be recalled is within a rectangle of size L centered in t'.

The mapping now proceeds as follows. In the continuum asymptotic case the memory's effective length L is given by (see Eq. (7) in Ref. [59])

$$L = \int_0^t [P_r(t',t)/P_{\max}(t)]dt', \tag{2}$$

where $P_{\max}(t)$ is the maximum value of $P_r(t',t)$. We prefer to work with the discrete version of Eq. (2), which reads

$$L = \sum_{t'=0}^{t} \frac{P_r(t',t)}{P_{\max}(t)}, \tag{3}$$

where $P_r(t',t)$ is given by Eq. (1). We can now infer $P_{\text{eff}}(t')$, namely the effective distribution of t', for large t. Note that $P_{\max}(t)$ is obtained for $t' = \lfloor (t+1)r \rfloor$, i.e., the largest integer smaller than $(t + 1)r$ {or, alternatively, $t' = \lceil (t+1)r \rceil - 1$}. For large t, the most probable memory value accessed is then given by $t' = rt$. In what follows we simply write $t' = \lfloor (t + 1)r \rfloor = (t + 1)r$ to avoid the use of cumbersome notation. It is easy, although burdensome, to show that

$$P_{\max} = \frac{1}{\sqrt{2\pi r(1-r)}} t^{-1/2}, \tag{4}$$

valid for large t. Using Eq. (3) we can now show that $L = \sqrt{2\pi r(1-r)}\, t^{1/2}$ in the asymptotic limit. Hence, the fraction of memory L/t that is effectively used, goes to zero for large t.

B. The δ memory profile

In the asymptotic limit, the effective distribution of t' in the binomial model, therefore tends to a δ function, i.e., $P_{\rm eff}(t') = \delta(t' - rt)$. In this case the walker remembers only a single point that moves with time. A continuous-time solution for the first moment of the δ memory pattern has already been provided before [52] along with an analytic expression for the Hurst exponent. As a function of the pair (p,r) an expression for H reads

$$H = \frac{\ln(|2p-1|)}{\ln(r^{-1})} + 1, \tag{5}$$

valid only in the superdiffusive regime. It was also shown that, in the asymptotic limit, the phase space (p,r) is divided in two regions separated by a parabola $r = 4p^2 - 4p + 1$, with two distinct regimes: superdiffusive below the parabola and normally diffusive above it. The δ memory profile model shows log-periodic oscillations for $p < 1/2$ (for any t), but no oscillations were found for $p > 1/2$. However, as we shall see below, the binomial memory model provides strong numerical evidence of log-periodic oscillations of small-amplitude for $p > 1/2$ and large times. We found out that the discrepancy between these two results relies on the fact that some of the fine structure of the discrete-time solution is lost in the continuous-time solution. We therefore carried out discrete-time calculations for the δ memory profile model. This is done below.

The δ memory model is simply defined by $P_{\rm eff}(t') = \delta(t' - rt)$, with t' set to an integer, as time is discrete. It is therefore convenient to set $t' = \lfloor rt \rfloor$, i.e., the largest integer smaller than rt. We look for a solution by writing down and solving the discrete-time equations. The walker's position at time t can be written as

$$X(t) = \sum_{j=0}^{t} \sigma(j), \tag{6}$$

where $\sigma(j) = \pm 1$ is the speed at time j, representing a stochastic noise containing two-point memory correlations. The initial condition is set by $\sigma(t=0) = 1$. An effective velocity at time t can be defined by $\sigma_{\rm eff}(t) = P^+(t) - P^-(t)$, where $P^+(t)$ and $P^-(t)$ are the probabilities of moving to the right and to the left, respectively, at time t. We now write

$$P^+(t) = pP^+(rt) + (1-p)P^-(rt)$$
$$P^-(t) = pP^-(rt) + (1-p)P^+(rt),$$

which sets $\sigma_{\rm eff}(t) = (2p-1)[P^+(rt) - P^-(rt)] = \alpha\sigma_{\rm eff}(rt)$, with $\alpha = 2p - 1$. As stated above, in this equation rt must actually be set as $\lfloor rt \rfloor$, i.e., the largest integer smaller than rt. A set of recursive relations can now be written as

$$\begin{aligned} \sigma_{\rm eff}(t) &= \alpha\sigma_{\rm eff}(rt) \\ \sigma_{\rm eff}(rt) = \alpha\sigma_{\rm eff}(r^2t) &\Rightarrow \sigma_{\rm eff}(t) = \alpha^2\sigma_{\rm eff}(r^2t) \\ \sigma_{\rm eff}(r^2t) = \alpha\sigma_{\rm eff}(r^3t) &\Rightarrow \sigma_{\rm eff}(t) = \alpha^3\sigma_{\rm eff}(r^3t), \end{aligned} \tag{7}$$

and so on. Note that this solution of the form $\sigma_{\rm eff}(t) \sim \alpha\sigma_{\rm eff}(rt)$ may lead to periodic solutions in $\ln(t)$ with period $\ln(1/r)$ [52,54]. From Eqs. (7) we can see that

$$\sigma_{\rm eff}(t) = \alpha^{N-1}\sigma_{\rm eff}(r^{N-1}t), \tag{8}$$

valid for some integer N. Using the initial condition $\sigma(0) = 1$ we can write $\sigma_{\rm eff}(1) = \alpha\sigma_{\rm eff}(0) = \alpha$ and determine N, since $\sigma_{\rm eff}(t) = \alpha\sigma_{\rm eff}(rt)$. Therefore the maximum integer N that solves Eq. (8) and satisfies the initial condition can be obtained by solving $r^{N-1}t = 1$.

From Eq. (6) we can write the first moment as

$$\langle X(t) \rangle = \sum_{t'=0}^{t} \langle \sigma(t') \rangle.$$

Just as we did for N in Eqs. (7) and (8), we can write a recurrence result for each t' as $\sigma_{\rm eff}(t') = \alpha^{(n_{t'}-1)}\sigma_{\rm eff}(r^{(n_{t'}-1)}t')$ such that $r^{(n_{t'}-1)}t' = 1$, and since $\sigma_{\rm eff}(1) = \alpha\sigma_{\rm eff}(0) = \alpha$, we get $\sigma_{\rm eff}(t') = \alpha^{n_{t'}}$. Therefore we can write the exact discrete-time solution for the first moment in the form

$$\langle X(t) \rangle = \sum_{t'=0}^{t} \alpha^{n_{t'}} \tag{9}$$

valid for any t. The asymptotic limit of Eq. (9) can be approached by defining $a_{t'} = \ln t'/\ln(1/r)$ for $t' \geqslant 1$ and $n_{t'} = \lfloor a_{t'} \rfloor + 1$. For $t' = 1$ we get $a_1 = 0$ and $n_1 = 1$. Note that $n_{t'}$ is constant within intervals m, with $n_{t'} = m$. Therefore $n_{t'}$ is a stepwise function that depends on $\ln t'$. This is, ultimately, the source of the log-periodic behavior for $\alpha > 0$ (or $p > 1/2$) as seen in Fig. 2(c). For example, for $r = 0.1$ and any p, the sum in Eq. (9) writes

$$\langle X(t) \rangle = 1 + 9\alpha + 99\alpha^2 + 999\alpha^3 + \mathcal{O}(\alpha^4), \tag{10}$$

where the unity represents $t' = 0$ and the α terms correspond, respectively, to t' within the intervals $1 \leqslant t' < 10$, $10 \leqslant t' < 100$, and $100 \leqslant t' < 1000$. Note that if $\alpha < 0$ $(p < 1/2)$ the terms alternate in sign giving rise to stronger oscillating behavior as in Fig. 2(b) (see below).

We can now use Eq. (9) to find the separating line between log-periodic and non-log-periodic behavior for $\alpha > 0$ $(p > 1/2)$. As discussed in Ref. [52] the asymptotic behavior can be written as $\langle X(t) \rangle \sim t^{\delta}$, where $\delta = \ln(|\alpha|/r)/\ln(1/r)$. Therefore we can write $\langle X(t) \rangle / t^{\delta} =$ log periodic correction terms. If $|\alpha|/r < 1$, then $\delta < 0$ and the log-periodic behavior of $\langle X(t) \rangle$ disappears for large t. We conclude that, below the line $|\alpha| = r$ or $r = 2p - 1$ $(p > 1/2)$, there is sustainable log-periodic behavior.

The discrete-time solution for the first moment unequivocally reveals the log-periodic modulations for $p > 1/2$, thus agreeing with the numerical results for the binomial memory model at large t.

III. RESULTS

Figure 1 shows the second moment $\langle x^2(t) \rangle$ as a function of time for the binomial model. Note that small and large values of the feedback parameter p favor superdiffusion (persistence) and small values for the pair (p,r) lead to strong log-periodicity. We can also determine the asymptotic value of the Hurst exponent using Eq. (5). For $(p,r) = (0.1,0.10)$ or $(p,r) = (0.9,0.10)$ we get $H \approx 0.903$, in excellent agreement with the numerical result shown in the figure. According to the figure, there is no explicit indication of log-periodicity for $p > 1/2$. In fact, as we shall see below, there are no log-periodic oscillations for $(p,r) = (0.6,0.80)$, but a more

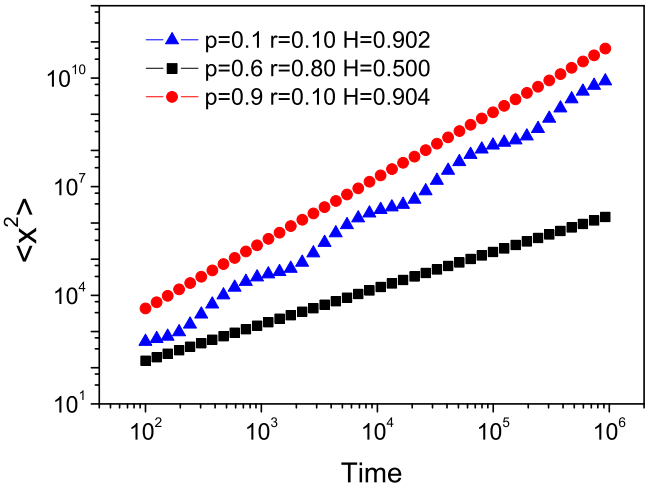

FIG. 1. Second moment as a function of time (10^6 runs with 10^6 total time units each) for several values for the Hurst exponent for the binomial model. Note that small and large values of the feedback parameter p favor superdiffusion (persistence). Negative feedback ($p < 1/2$) is known to lead to log-periodicity when the memory is damaged, as suggested by the steady oscillations in the $(p,r) = (0.1,0.10)$ curve. There is no log-periodic behavior associated with the pair $(p,r) = (0.6,0.80)$, as correctly implied by the corresponding straight line curve. However, the pair $(p,r) = (0.9,0.10)$ does lead to log-periodicity, contrariwise to what is indicated by the red solid circles straight line curve [see also Fig. 2(c) below].

careful analysis concludes that the second moment versus time curve for $(p,r) = (0.9,0.10)$ hides log-periodic modulations that are carried out to infinitely large t, as discussed below.

Figures 2(a)–2(d) show the behavior of the first moment $\langle x(t) \rangle$ for suitable choices of the model parameters and large t. It is worthwhile to note that persistent (superdiffusive) regimes for $p \gg 1/2$ are expected because large p implies that earlier decisions are repeated very often, ultimately leading to superdiffusion. Damaged memory, as in denying access to recent memories, also leads to superdiffusion, this time for $p \ll 1/2$. Log-periodicity is, in fact, expected for $p < 1/2$ according to previous results [46]. Note also that normal diffusion is always favored for $p \approx 1/2$. On the other hand, large values of r are associated to recent memories which are related to normal diffusion. Therefore, different pairs (p,r) represent competitive effects with respect to the resulting type of diffusion obtained in the asymptotic limit. These comments can be fully appreciated in Figs. 2(a)–2(d). According to Fig. 2(a), the binomial model exhibits log-periodicity within the negative feedback region ($p < 1/2$), as discussed above. Notice the large values for the Hurst exponent, due to the small values of the pair (p,r). Figures 2(b) and 2(c) show $\langle x \rangle / t^H$ curves for large p. Here we notice a totally unexpected log-periodic behavior appearing in a positive feedback region ($p > 1/2$). Notice, in particular, the oscillating curve $\langle x \rangle / t^H$ for $(p,r) = (0.9,0.10)$ depicted in Fig. 2(c). This should be compared with the straight line for the second moment shown in Fig. 1. Here, when divided by t^H, we can see the oscillations more clearly. However, in some cases it can be misleading, even with the normalization factor t^H, as can be seen in the top curves of Figs. 2(b) and 2(c). Note the small amplitude of the oscillations for $p > 1/2$. These oscillations represent log-periodic corrections to the coefficient of the time expansion of the first moment. Despite their small amplitude, the oscillations are real and do not disappear for large times. In fact, we carried out exhaustive computing experiments with different random number generators for larger time ensembles, showing that these oscillations are not an artifact of numerical noise. In order to prove that the oscillations are sustained even for large times, we consider the pair $(p,r) = (0.9,0.05)$ represented by the solid black squares in Fig. 2(c) and treated the data separately in Fig. 2(d). The main figure shows the first moment for the binomial memory profile model, obtained by careful numerical analysis and normalized by $t^{1/2}$. This normalization factor is enough to uncover log-periodic oscillations in this case. However, the curve is still a monotone increasing function of $\ln(t)$ with no signs of oscillations. The same data are shown at the top of the inset, this time properly normalized by t^H using the numerical value for the Hurst exponent, i.e., $H = 0.92565$, from Fig. 2(c). The inset also shows the exact first moment for the δ memory profile model obtained using Eq. (9) and properly normalized by t^H [with $H = 0.92551$ from Eq. (5)]. We see that the binomial model tends to the δ memory model for large times, as noted above. The figures are adjusted so that the two first peaks coincide. It is seen that both first moments oscillate with the same frequency. Since the oscillations for the δ memory model never disappear, we conclude that the oscillations in the binomial model are sustained indefinitely.

Figure 3 shows the phase diagram r versus p exhibiting the values for the Hurst exponent H. The parabola $r = 4p^2 - 4p + 1$, shown as a thick solid black line, separates the superdiffusive ($H > 1/2$, below the parabola) regime from the normally diffusive ($H = 1/2$, above the parabola) regime in the asymptotic limit. Apart from the parabola, derived from the continuous-time solution for the δ memory pattern [52], all regions were obtained numerically. This diagram provides a good representation of the regime transitions that occur as one crosses over regions with different values of H. The numerical results indicating $H > 1/2$ above the parabola are just finite-size effects, possibly representing a transient superdiffusive regime that must disappear for large t [60,61]. Log-periodic oscillations occur below the black dashed line (see text). Note that log-periodicities occur even for $H = 1/2$, as in the region between the dashed line and the parabola. As emphasized above, the modulations are somewhat expected for strongly correlated damaged memory systems when associated with negative feedback regimes [61]. However, their appearance within the positive feedback region ($p > 1/2$) of the phase diagram could not be foreseeable beforehand. As far as we know, they are totally unknown and unexpected.

Although the general conditions for the onset of log-periodicity are still unclear, one can understand their origin reasonably well in stochastic random-walk memory models. For these models, the emergence of log-periodic modulations are associated with the loss of memory of the recent past and have only been reported for $p < 1/2$. The loss of memory of the recent past characterizes an inability to create new memories and is a medical condition known in the specialized literature as anterograde amnesia. In the stochastic model, the modulations appear because, when only the long distant memories are available to the walker, the effect of

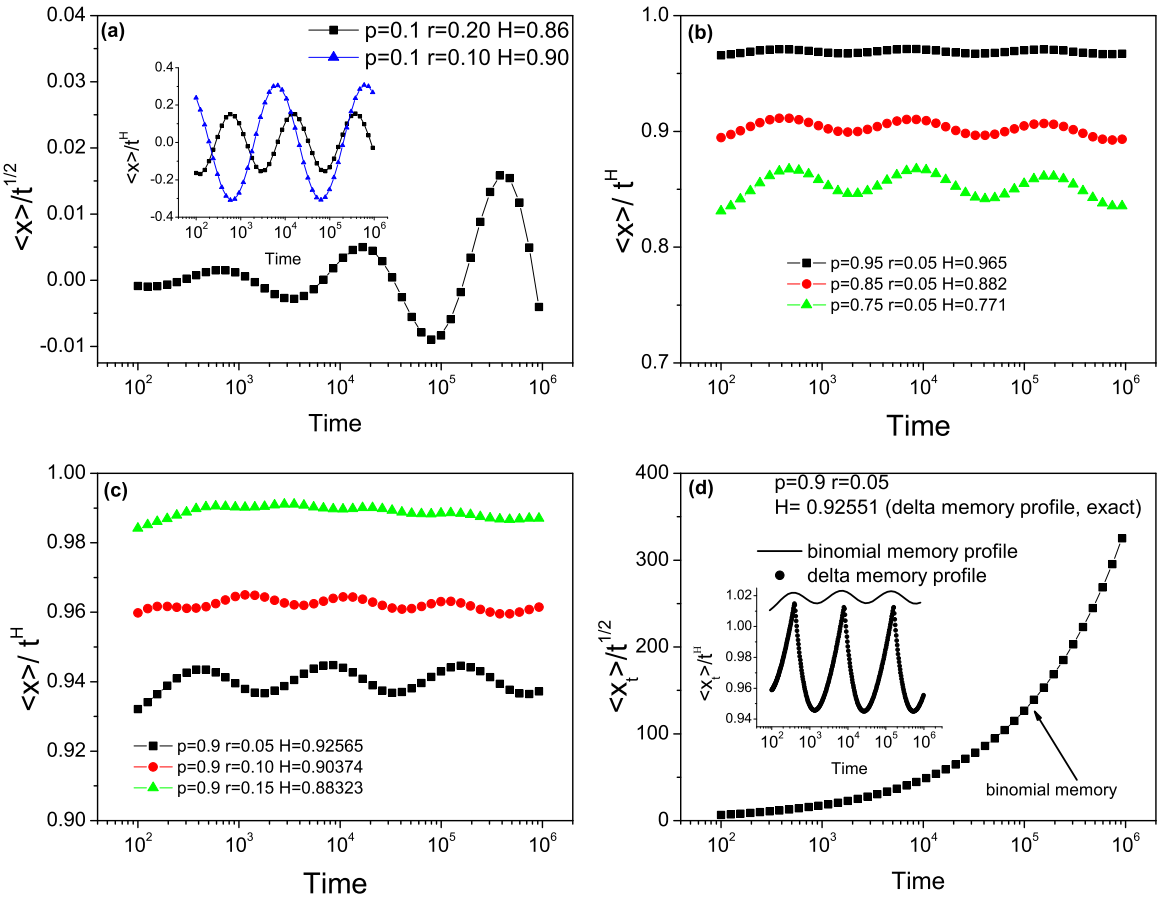

FIG. 2. Behavior of the first moment for suitably chosen pairs (p,r) within regimes displaying log-periodic oscillations (numerical simulations with 10^6 runs and 10^6 total time units each). (a) shows superdiffusive regimes ($H > 1/2$) for small values of p and r for the binomial model. The normalization factor $t^{1/2}$ is usually fine to expose log-periodicity as seen in the main figure. The inset shows the effect of a more convenient normalization factor, namely t^H, along with another pair (p,r). Panels (b) and (c) exhibit the expected superdiffusive behavior for $p \gg 1/2$ for the binomial model. The small amplitude oscillations against $\ln t$ indicate nonexpected log-periodic modulations. (d) compares the oscillations for the first moment for both the binomial model (numerical) and the δ memory model (exact).

the action taken at the present time t only enters into the range of the accessible memory after a time delay [46]. This leads to superdiffusion, even for $p < 1/2$, and generates alternate persistence windows in the first moment (i.e., steps predominantly in a given direction) that grow exponentially in time and ultimately producing log-periodicity. Log-periodic modulations are a signature of DSI [51] while classical, non-log-periodic, persistence is indicative of CSI. DSI is associated with discrete values of the magnification factor [62,63] and is characterized by complex scaling exponents. The presence of log-periodicity therefore implies that CSI in the binomial memory model can be spontaneously broken. It is therefore an important practical problem to be able to acknowledge their presence and understand their origins.

Another important point to emphasize is the difference between the discrete-time solution and the continuous-time solution (CTS) for the δ memory profile model. As discussed above, the CTS we provide reproduces correctly the log-periodicities for $\alpha < 0$, but it is not capable of displaying the small-amplitude log-periodic oscillations for $\alpha > 0$. The discrete-time solution does not suffer from this limitation. It is important to emphasize that the continuous-time "solution," as derived before [52], was obtained by taking the continuous-time limit of a discrete time equation, namely the derivative of the first moment of the δ memory model. This solution was not meant to represent a continuous-time "model" solution, as if it were derived from, say, the CTRW or similar model (see Ref. [64] for a CTRW formulation of the original ERW model). Note, however, that the binomial or δ memory models use a microscopic approach to model memory, which is not immediately translated into correlated random noise terms to be used in continuous-time models (CTRW, Langevin and Fokker-Planck equations, etc.). This would be an interesting contribution to the study of these RW models, a task that is greatly complicated by the strong non-Markovian nature of these processes.

IV. DISCUSSION AND CONCLUSION

We employed a binomial distribution to characterize a memory profile to study the effect of long-time memory correlations in random-walk diffusion. Log-periodic corrections to scaling were found in the negative feedback region of the phase diagram, in accordance with previous studies. However, log-periodic oscillations were also found, this time in

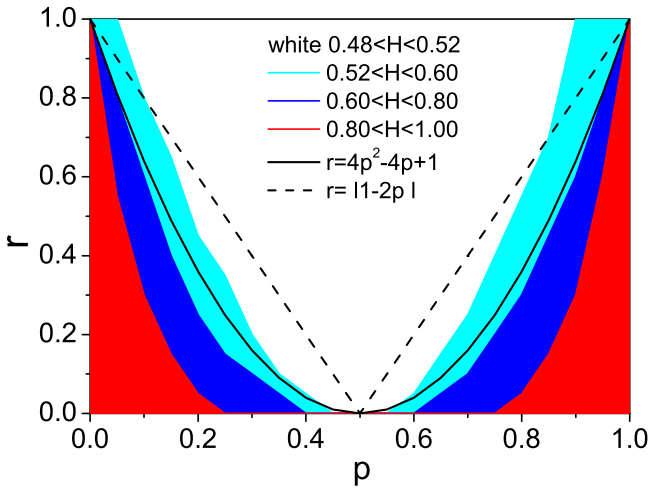

FIG. 3. Phase diagram r versus p, showing several regions depicting the values for the Hurst exponent H and separating regions where log-periodic behavior occurs. The colored regions represent numerical results obtained with 10^6 runs with 10^6 total time units each. The parabola $r = 4p^2 - 4p + 1$ separates the superdiffusive regime ($H > 1/2$) from the normally diffusive regime ($H = 1/2$) in the asymptotic limit. The values for $0.52 < H < 0.60$ found above the parabola are due to finite-size effects. The region below (above) the parabola is superdiffusive (normally diffusive). The region below (above) the black dashed line is log-periodic (non-log-periodic).

a nonexpected positive feedback region of the phase diagram. Nonetheless, these oscillations are of very small amplitude, almost indistinguishable from numerical size effects, thus raising the question of whether they are real and/or sustained in the large-time limit. Fortunately, the binomial profile tends to a δ memory pattern for large times. Therefore, in the absence of an analytical solution for the binomial memory profile model, we settle to establish the existence of the oscillations by examining the asymptotic behavior of the δ memory profile model. It was then shown that, as a result of discrete-time effects, log-periodic modulations of very small amplitude emerge in the positive feedback region of the phase diagram of the δ memory, which are then carried out to the asymptotic limit, never disappearing. This result unmistakably eliminates any doubts on the existence of large-time positive feedback log-periodic modulations as displayed by the binomial model. We also conclude that, while negative feedback enhances the oscillation amplitudes and clearly exposes the log-periodic behavior, positive feedback may lead to oscillations of very small amplitude, which can easily be mistaken for finite-size numerical effects. For superdiffusive regimes it is advisable to plot $\langle X_t \rangle / t^H$ against $\ln t$ in order to be able to spot these oscillations. We are confident that such subtle log-periodic oscillations appear in many other systems with damaged memories. Some previously published papers might need to be reviewed. On the other hand, it becomes also clear from this study that continuous-time solutions may hide oscillations due to memory damage, since they interpolate between the successive time windows that are incorporated into memory as time evolves.

ACKNOWLEDGMENTS

We thank G. M. Viswanathan for his careful reading of the manuscript and important suggestions. We also thank the High Performance Computing Center at UFRN for providing the computational facilities to run the simulations. J.C.C. and M.A.A.S. acknowledge FAPESP (Grants No. 2011/13685-6, No. 2011/06757-0, No. 2016/03908-7, and No. 2017/01176-6) for financial assistance. M.A.A.S. thanks CNPq (Grant No. 308280/2015-6) for funding.

[1] P. Hänggi, F. Marchesoni, and F. Nori, Ann. Phys. **14**, 51 (2005).
[2] R. Brown, Philos. Mag. Ser. 2 **4**, 161 (1828).
[3] A. Einstein, Ann. Phys., Lpz. **322**, 549 (1905).
[4] M. von Smoluchowski, Ann. Phys., Lpz. **326**, 756 (1906).
[5] P. Hänggi and F. Marchesoni, Chaos **15**, 026101 (2005).
[6] J. Fourier, *Théorie analytique de la chaleur* (Firmin Didot Père et Fils, Paris, 1822).
[7] A. Fick, Poggendorff's Ann. Phys. **170**, 59 (1855).
[8] L. Bachelier, Ann. Sci. École Norm. Sup. **17**, 21 (1900).
[9] K. Pearson, Nature **72**, 342 (1905).
[10] G. H. Weiss, *Aspects and Applications of the Random Walk* (North-Holland, Amsterdam, 1994).
[11] E. Nelson, *Dynamical Theories of Brownian Motion* (Princeton University Press, Princeton, NJ, 1967).
[12] J. Klafter, M. F. Shlesinger, and G. Zumofen, Phys. Today **49**, 33 (1996).
[13] R. Metzler and J. Klafter, Phys. Rep. **339**, 1 (2000).
[14] S. Sharma and Vishwamittar, Resonance **10**, 49 (2005).
[15] J. Klafter and I. M. Sokolov, Phys. World **18**, 29 (2005).
[16] V. Zaburdaev, S. Denisov, and J. Klafter, Rev. Mod. Phys. **87**, 483 (2015).
[17] P. Mörters and Y. Peres, *Brownian Motion* (Cambridge University Press, New York, 2010).
[18] W. T. Coffey and Y. P. Kalmykov, *The Langevin Equation: With Applications to Stochastic Problems in Physics, Chemistry, and Electrical Engineering* (World Scientific, Singapore, 2012).
[19] R. Kubo, M. Toda, and N. Hashitsume, in *Statistical Physics II* (Springer, Berlin, 1985), Vol. 31.
[20] K. Lindenberg and B. J. West, *The Nonequilibrium Statistical Mechanics of Open and Closed Systems* (VCH, New York, 1990).
[21] H. Mori, Prog. Theor. Phys. **34**, 399 (1965).
[22] E. W. Montroll and G. H. Weiss, J. Math. Phys. **6**, 167 (1965).
[23] H. Scher and E. W. Montroll, Phys. Rev. B **12**, 2455 (1975).
[24] R. Metzler, E. Barkai, and J. Klafter, Phys. Rev. Lett. **82**, 3563 (1999).
[25] E. Barkai, Phys. Rev. E **63**, 046118 (2001).
[26] I. Eliazar and J. Klafter, Phys. Rev. Lett. **103**, 040602 (2009).

[27] R. N. Mantegna and H. E. Stanley, *An Introduction to Econophysics: Correlations and Complexity in Finance* (Cambridge University Press, Cambridge, 1999).
[28] A. Pekalski and K. Sznajd-Weron (eds.), *Anomalous Diffusion: From Basics to Applications*, Vol. 519 of Lecture Notes in Physics (Springer-Verlag, Berlin, 1999).
[29] R. Metzler and J. Klafter, J. Phys. A: Math. Gen. **37**, R161 (2004).
[30] C. Nicolis and G. Nicolis, Phys. Rev. E **80**, 061119 (2009).
[31] R. J. Harris and H. Touchette, J. Phys. A **42**, 342001 (2009).
[32] S. Havlin and D. Ben-Avraham, Adv. Phys. **36**, 695 (1987).
[33] M. Grifoni and P. Hänggi, Phys. Rep. **304**, 229 (1998).
[34] M. F. Shlesinger, G. M. Zaslavsky, and J. Klafter, Nature **363**, 31 (1993).
[35] R. Kutner, A. Pękalski, and K. Sznajd-Weron (eds.), *Anomalous Diffusion: From Basics to Applications* (Springer, Berlin, 1999).
[36] R. Golestanian, Phys. Rev. Lett. **102**, 188305 (2009).
[37] P. Brault, C. Josserand, J. M. Bauchire, A. Caillard, C. Charles, and R. W. Boswell, Phys. Rev. Lett. **102**, 045901 (2009).
[38] A. Mertelj, L. Cmok, and M. Copic, Phys. Rev. E **79**, 041402 (2009).
[39] Y. G. Sinai, Theor. Probl. Appl. **27**, 256 (1982).
[40] S. Havlin, A. Bunde, Y. Glaser, and H. E. Stanley, Phys. Rev. A **34**, 3492 (1986).
[41] D. Cassi and S. Regina, Phys. Rev. Lett. **76**, 2914 (1996).
[42] J. Dräger and J. Klafter, Phys. Rev. Lett. **84**, 5998 (2000).
[43] M. A. A. da Silva, G. M. Viswanathan, and J. C. Cressoni, Phys. Rev. E **89**, 052110 (2014).
[44] S. Fedotov and Y. Okuda, Phys. Rev. E **66**, 021113 (2002).
[45] G. M. Schütz and S. Trimper, Phys. Rev. E **70**, 045101 (2004).
[46] J. C. Cressoni, Marco Antonio Alves da Silva, and G. M. Viswanathan, Phys. Rev. Lett. **98**, 070603 (2007).
[47] N. Kumar, U. Harbola, and K. Lindenberg, Phys. Rev. E **82**, 021101 (2010).
[48] U. Harbola, N. Kumar, and K. Lindenberg, Phys. Rev. E **90**, 022136 (2014).
[49] H.-J. Kim, Phys. Rev. E **90**, 012103 (2014).
[50] R. Kürsten, Phys. Rev. E **93**, 032111 (2016).
[51] D. Sornette, Physics Reports **297**, 239 (1998).
[52] J. C. Cressoni, G. M. Viswanathan, A. S. Ferreira, and M. A. A. da Silva, Phys. Rev. E **86**, 022103 (2012).
[53] D. Stauffer and D. Sornette, Physica A **252**, 271 (1998).
[54] W. J. Reed and B. D. Hughes, Phys. Rev. E **66**, 067103 (2002).
[55] W. J. Reed and B. D. Hughes, Physica A **319**, 579 (2003)
[56] S. Gluzman and D. Sornette, Phys. Rev. E **65**, 036142 (2002).
[57] B. Derrida and G. Giacomin, J. Stat. Phys. **154**, 286 (2014).
[58] G. M. Borges, A. S. Ferreira, M. A. A. da Silva, J. C. Cressoni, G. M. Viswanathan, and A. M. Mariz, Eur. Phys. J. B **85**, 1 (2012).
[59] G. A. Alves, J. M. de Araújo, J. C. Cressoni, L. R. da Silva, M. A. A. da Silva, and G. M. Viswanathan, J. Stat. Mech. (2014) P04026.
[60] T. R. Moura, G. Viswanathan, M. da Silva, J. Cressoni, and L. da Silva, Physica A **453**, 259 (2016).
[61] J. C. Cressoni, M. A. A. da Silva, and G. M. Viswanathan, Physica A **364**, 70 (2006).
[62] B. B. Mandelbrot, *The Fractal Geometry of Nature* (Freeman, San Francisco, CA, 1982).
[63] S. Havlin and A. Bunde, in *Fractals and Disordered Systems* (Springer, Berlin, 1991), pp. 97–150.
[64] F. N. C. Paraan and J. P. Esguerra, Phys. Rev. E **74**, 032101 (2006).